

# Wide-angle X-ray Scattering studies on contemporary and ancient bast fibres used in textiles – ultrastructural studies on stinging nettle

Mira Viljanen (✉ [mira.viljanen@helsinki.fi](mailto:mira.viljanen@helsinki.fi))

University of Helsinki Faculty of Science: Helsingin yliopisto Matemaattis-luonnontieteellinen tiedekunta  
<https://orcid.org/0000-0003-0654-1011>

Jenni Suomela

University of Helsinki: Helsingin Yliopisto

Kirsi Svedström

University of Helsinki Faculty of Science: Helsingin yliopisto Matemaattis-luonnontieteellinen tiedekunta

---

## Research Article

**Keywords:** Nettle, Plant fibre, Ultrastructure, Wide-Angle X-ray Scattering

**Posted Date:** April 27th, 2021

**DOI:** <https://doi.org/10.21203/rs.3.rs-231060/v1>

**License:**  This work is licensed under a Creative Commons Attribution 4.0 International License.

[Read Full License](#)

---

**Version of Record:** A version of this preprint was published at Cellulose on January 24th, 2022. See the published version at <https://doi.org/10.1007/s10570-021-04400-w>.

# Abstract

Stinging nettle (*Urtica dioica*) among other bast fibres, is a potential fibre source material for industrial and manufacturing applications. However, systematic research on the ultrastructural properties of nettle fibres is lacking. Determining the ultrastructural parameters of the bast fibres could provide also new insights into the studies of archaeological and historical fibres and their usage.

In this study, modern and ancient fibre samples of stinging nettle were studied using wide-angle X-ray scattering (WAXS) and compared to other well-studied plant fibre species. From the WAXS patterns, the mean microfibril angle, average cellulose crystallite width and relative crystallinity index were determined.

Besides, the suitability of the WAXS method for fibre identification purposes was studied. The culturohistorical research material consisted of fibre samples of nettle, flax and hemp acquired from White Karelian textiles collected 1894 as well as of 800–900-year-old archaeological textile fragments from Ravattula Ristimäki burial site in Kaarina, Southwest Finland.

The crystallite widths for all modern fibres were of the similar size, however subtle differences in the relative crystallinity values in descending order (from flax to nettle and finally hemp) were observed. For the culturohistorical fibres, the values for average crystallite width and relative crystallinity were larger compared to the modern references of the same fibre type. In addition, individual features due to the presence of other crystalline substances (noncellulosic, minerals e.g., calcium oxalates), were detected in the scattering patterns of all modern nettles. These features could potentially be used as a tool to identify modern nettle fibres.

## Introduction

Plant fibres have been used in clothing, tools and decorations since early days of human history due to their accessibility, processability and great mechanical properties. The most common plant fibres used in the textile making in the Northern Hemisphere are flax (*Linum usitatissimum*), hemp (*Cannabis sativa*) and stinging nettle (*Urtica dioica*) (Geijer 1979). Perhaps one of the most important fibres for craftsmanship has been stinging nettle: it is the only indigenous fibre producing species in Scandinavia, thus it has been used as textile fibre before the arrival of the other plant fibres (Suomela et al. 2020). Even today, with greater than ever increasing need of sustainable and durable textile-making materials, nettle derived fibres could potentially prove out to be promising candidates for the purpose. For that, the ultrastructural properties of nettle fibres need to be studied in more detail.

Nettle fibres, like flax and hemp, are derived from the plant stem (*bast fibres*), consisting of elongated, dead sclerenchyma cells. These cells function as supportive tissue of the plant due to their cell wall structure and thickness (Sfiligoj et al. 2013). Inside the cell walls, the cellulose chains are accumulated into partially crystalline microfibrils, embedded into a hemicellulose-lignin matrix. The properties and orientation of the microfibrils are significant as they affect to the strength and stiffness of the whole plant (Reiterer et al. 1999).

The cellulose microfibrils are helically oriented around the cell lumen, forming a certain angle with the vertical axis of the cell, known as the *microfibril angle*. In primary cell wall, the orientation of the microfibrils is random counter to the secondary cell walls in which the microfibrils are highly orientated within each three sublayers. The whole fibre is said to be orientated with a Z-twist if the microfibrils in the thickest sublayer of the secondary cell wall twist to the right, while the opposite case (left-handed twist) fibrillar orientation is known as S-twist. A modified Herzog test or the red plate test is utilised to determine the twist direction (S- or Z-twist) (Haugan and Holst 2013).

Stinging nettle belongs to the family of *Urticaceae* as the more studied ramie (*Boehmeria nivea*). As a wide-spread plant in the wild, nettle requires almost no extra watering or care, making it a biodegradable source for fibre production (Markova 2019). This ecological aspect combined with other advantageous traits like nontoxicity, processability and recyclable have contributed to the popularity and increasing utilization of nettle fibres and yarn products (Debnath 2015). Nowadays, the interest in plant fibres and fibre formed structures does not only limit to textiles as some common plant fibres have turned out to be very functional materials for biocomposites due to their great mechanical properties (Ramamoorthy et al. 2015). Alongside other well-studied plant fibres (Sanjay et al. 2019) nettle has been increasingly researched to determine its suitability to be used as a composite material (Kumar and Das 2017b; Viju and Thilagavathi 2020).

For textile making purposes, it has recently been suggested that nettle textiles were used more broadly and commonly in the history than previously assumed (Bergfjord et al. 2012; Vajanto 2014; Suomela et al. 2018; Suomela et al. 2020). In fibre research, nettle fibres have often been overlooked by flax and hemp, leading to false identification of the fibres and wrong assumptions of the used plants for craftsmanship. Identification of bast fibres (flax, nettle and hemp) is still challenging with existing methodologies, even though urge for reliable results include various fields from archaeology to criminology (Deedrick 2000).

From the archaeological point of view, even single fibres or their physical traces can provide useful information about the cultural context. Textile fibre findings can all potentially contribute to the knowledge of the used materials, techniques, and skills required to make the item as well as past social environments, migration of inhabitants and ancient trade routes (Good 2001).

The fibrillar orientation (S- or Z-twist) is one of the key features of interest when it comes to identifying the bast fibres from modern and archaeological textiles. For the identification studies of plant fibres, commonly used techniques include transmission light microscopy (TLM) and polarized light microscopy (PLM) to observe the surface characteristics and other distinctive properties of the fibres. In addition, the cross-sectional characteristics of the fibres (Suomela et al. 2018) and traces of single mineral crystals or crystal clusters (*druses*) in the fibre associated tissue (Bergfjord and Holst, 2010) are also studied. These crystals and druses are mainly compounds of calcium derived oxalates and carbonates, formed into a certain crystallographic structure (Fengel and Wegener 1983; Webb 1999), and are observable in PML, depending on their sizes and the resolution of the used equipment. In addition, these crystals and clusters

can be studied further using scanning electron microscopy (SEM) (Markova 2019) and plasma-ashing (Jakes and Mitchell 1996).

An example of fibre identification study which benefits from combining all the above-mentioned fibre features is the case of separating flax and nettle fibres: they share the same fibrillar orientation (Bergfjord and Holst 2010) but have very different and distinctive cross-sectional shapes (Nayak et al. 2012; Suomela et al. 2018; Lanzilao et al. 2016). Additionally, oxalate crystals and clusters have been reported not to be detected in flax fibres (Catling and Grayson 1982; Bergfjord and Holst 2010).

The traditional TML and PLM measurements, limited to the micrometer resolution, conducted on the fibre samples do not provide information about the ultrastructural properties i.e., the structures of the cellulose microfibrils. Conducting X-ray Diffraction (XRD) and scattering measurements on the fibre samples of interest, it is possible to obtain information on the atomic and nanoscale arrangement of cellulose in the samples. XRD and Wide-Angle X-ray Scattering (WAXS) can be used to determine the amount of crystalline cellulose of the total weight of the sample and the size and orientation of the cellulose crystallites in the cellulose microfibrils. By comparison of the ultrastructural properties of the cellulose microfibrils, it is possible to characterize the condition of cellulose in the fibre samples (Müller et al. 2007).

X-ray scattering and diffraction methods are widely used to study the nanoscale properties of cellulose-based materials, because they are considered as non-destructive i.e., the methods do not often require any chemical treatment or sectioning of the samples. From the archaeological point of view, the non-destructive research methods that only need small amount of sample, are highly desirable. X-ray scattering and diffraction techniques are relatively unused but promising methods to be applied on the structural studies of archaeological and modern fibres (Müller et al. 2004; Müller et al. 2006; Müller et al. 2007).

In this study, various modern and historical samples of stinging nettle, flax, hemp and cotton were studied using WAXS and traditional microscopy methods (PLM & TLM). The aim of the research was to gain information about the structural properties of cellulose microfibrils in nettle bast fibres in contrast of the well-studied species (flax, hemp, cotton). It should be noted that there are only few previous home laboratory XRD studies conducted on archaeological fibres (Chen et al. 1998). Besides, only a couple of studies have focused on the structural properties of pure nettle textile fibres (Bergfjord and Holst 2010; Bergfjord et al. 2012; Kumar and Das 2017a; Lanzilao et al. 2016) and no systematic research especially on the ultrastructural characteristics of cellulose microfibrils in nettle in comparison with the other well-studied fibrous species have been previously made. Thus, this research reveals novel ultrastructural information on both regarding the structural properties of stinging nettle and the cellulose structure state of the unique archaeological and historical bast fibres included in this study.

## Materials

For the study, different types of modern (reference) and culturohistorical (ethnographic and archaeological) bast fibre samples were measured using WAXS. The ethnographic samples were classified as nettle, flax or hemp based on the previously published TLM and PLM results (Suomela et al. 2020). In addition, three archaeological fibre samples were measured using WAXS to be used as a comparative result as well as to test the method's practicality to study degraded samples. The TLM/PLM results of these archaeological fibres are published in a separate article (Suomela et al. *In preparation*)

The studied reference samples belonged to species and subspecies of stinging nettle, hemp and flax (Table S1 in supplementary). These reference samples have been classified by location of the fibres in plant (root/stem/crown), by collection time and by detachment method of the fibres. These methods simulated traditional practices to remove fibres from surrounding plant tissues. Some fibres were detached from dried stems, and some were water-retted in a bucket. Different detachment methods were applied to see if it had influence on the structure or characteristics of the fibres.

Culturohistorical samples consisted of ethnographic and archaeological samples from two separate sources. Ethnographic samples are from the Finno-Ugric Collection SU4522 of National Museum of Finland. The samples were extracted from linen textiles collected in 1984 from the White Karelian region, Russia, and have been stored in stable museum conditions since. These textiles represent the materials from the 18th and 19th century and are profoundly presented in Suomela et al., 2020. Details of the samples can be found in the supplementary material from table S2.

The archaeological samples consisted of small textile fragments, excavated from burial ground located in Ravattula Ristimäki in Kaarina, Finland. Ravattula, Ristimäki has been an active excavation site (2010 to 2016) of the Department of Archaeology in the University of Turku. The site consists of semi-Christian and Christian inhumation cemetery with the oldest know Christian church in Finland. The burial ground has been dated to be used approximately from the 12<sup>th</sup> century to the early 13<sup>th</sup> century. As an archaeological period, this timeline falls to end of the Crusade period (Ruohonen 2017). A detailed optical microscopy and x-ray microtomography studies of the Ravattula samples will be included in a separate article (Suomela et al. *in preparation*). Before the any of the conducted studies, the samples have been stored in Eppendorf-tubes in room temperature and normal moisture conditions. Additional details of the samples can be found in the supplementary material from table S3.

All the studied archaeological samples were found from different graves and within the proximity of possible bronze and silver containing items, i.e., sheath of a knife (sample TYA 912:523D) and a bracelet (sample TYA 914:1607:8A). Third sample was found from the upper body area with close contact with a glass bead and next to a silver coin (sample TYA 933:214:9:50).

## Methods

### *Optical microscopy measurements*

In this study, the microstructural characteristics are revealed for the chosen ethnographic samples representing each bast fibre type (nettle, hemp, flax) and their differences using TLM and PLM.

All the ethnographic fibre samples were identified in the previous study (Suomela et al. 2020) using the three-stage procedure introduced and explained in detail by Suomela et al. (2018). The procedure includes observation of longitudinal and cross-sectional characteristics with TLM and determination of the microfibrillar orientation with the Modified Herzog test using PLM. Based on these results, the samples were identified to either be originated from nettle, hemp, flax or cotton, with the fibre type noted in the Table 2 and Table S2 (supplementary).

### ***WAXS measurements and analysis***

The mean microfibril angle (MFA), average width of the cellulose crystallites and the relative fraction of the crystalline cellulose (relative crystallinity) of fibre samples were studied using wide-angle x-ray scattering (WAXS). The WAXS measurements were conducted in the X-ray laboratory at the University of Helsinki using a custom-built measurement setup with perpendicular transmission geometry mode. The X-rays were produced by a conventional copper x-ray tube, powered by generator (Seifert) using current and voltage of 25 mA and 36 kV, respectively. A Montel multilayer monochromator (Incoatec) was used to select the corresponding Cu K $\alpha$  radiation ( $\lambda = 1.541 \text{ \AA}$ ) and the scattered intensities were collected onto a MAR345 2D image plate detector (Marresearch).

A sample of lanthanum hexaboride (LaB<sub>6</sub>) was used to calibrate the scattering angle  $2\theta$  -range and to obtain the value of instrumental broadening, which was determined to be approximately 0.3 °. The samples were measured as dry either in air or as placed between two mylar foils in a washer. The measurement time was 42-60 minutes due to the extremely small amount of the sample material.

The WAXS data was analysed using Matlab. The data were corrected for background scattering arising from air and mylar foils by subtracting the background measured by using an empty sample holder covered with two mylar foils. The absorption, geometrical and polarization corrections were applied to the data. The transmission values for absorption correction, which was conducted before the background subtraction, were determined from the primary beam by using a semi-transparent copper beam stop.

The data was integrated using a 50° -wide sector (for crystallite width analysis) and a 180° -wide sector (for relative crystallinity analysis) around the cellulose 200 reflection in the two-dimensional scattering pattern. From the integrated data, the average width of the cellulose crystallites (crystallite size) and the relative amount of crystalline cellulose (crystallinity) in the samples were determined.

For the microfibrillar angle analysis of the modern fibres, an azimuthal integration over 180° -wide sector around the cellulose 200 reflection was carried out in a similar way than described in (Sarén et al. 2004). Using the azimuthal profile for a complete fibre sample (i.e., signal arising from both the front and rear walls), it is not possible to determine whether the fibre has Z- or S- twist, as the microfibrils are helically wound around the cells.

The average crystallite size was obtained using the Scherrer equation and similar curve fitting method with 4 or 5 Gaussians as described in detail in (Svedström et al. 2012), implemented around the 200 reflection, which in this dataset corresponds to the  $2\theta$  -range from 12° to 28°. In the case of the modern,

untreated samples of nettle and hemp, 4 Gaussian peaks were used in the curve fitting process while for the rest of the fibre samples (excluding the Ravattula TYA 912 sample), 5 Gaussians were used to generate the average crystallite sizes. Due to the extremely low scattering intensity acquired for the sample TYA 912, the average crystallite width has been computed by approximating the FWHM of the 200 reflection (without Gaussian fitting) and using the Scherrer equation.

For the modern and ethnographic bast fibre samples, the relative crystallinity was determined using the *amorphous fitting method* reported in (Ahvenainen et al. 2016). The scattering contribution from the amorphous components of cell wall was taken into account by using an amorphous standard, measured from sulphate-lignin (Andersson et al. 2003).

## Results

Here we present examples of the microscale structures often found in the studied fibres of flax, hemp and nettle. The presented examples are nonpublished TML and PML images of the White Karelian fibres, and complementary results can be found in (Suomela et al. 2020).

Regarding the ethnographic flax fibres (Sample 5a, Figure 1a), sparse cross markings and narrow lumen were detected. Cross-sectional observations were done using table glue methods (Suomela et al. 2020). The characteristic polygonal structure and small lumens typical for flax fibres could be detected in the images (Figure 1b). We also used modified Herzog test to study the fibrillar orientation which resulted a twist in S-direction (Figure 1 c<sup>1</sup> and c<sup>2</sup>).

In the longitudinal observation of nettle fibres (Sample 9b, Figure 2a), typical cross-markings and dislocations were observed. From cross-section images (Figure 2b), it was possible to detect kidney-shaped structures with flatten lumens. Using modified Herzog test, colour features similar to observed in flax fibres were detected, thus the fibrillar orientation was determined to be S (Figure 2 c<sup>1</sup> and c<sup>2</sup>).

The only ethnographic hemp sample 73ba had typical cross-markings and dislocations for bast fibres (Figure 3a). In the cross-sectional image (Figure 3b), circular shaped large lumens were visible, yet polygonal and kidney-shaped forms were also detected. Nevertheless, in case of hemp, the identification can be grounded on the modified Herzog test which clearly shows opposite twist to flax and nettle (Figure 3 c<sup>1</sup> and c<sup>2</sup>).

### **WAXS results**

We studied the cellulose crystallite widths and relative amount of crystalline cellulose of the cellulose microfibrils of the fibre samples using a laboratory X-ray scattering equipment, in which the size of the used X-ray beam was of the scale of 1 mm. The size of the measured fibres varied from 1-mm-thick clusters (reference samples) and microscopical pieces of fabric grids (archaeological samples) down to a minimum of 100- $\mu$ m-thick bundles (ethnographical samples), and the measured parameters are average values across the whole sample (considering the beam size, a corresponding area within the sample is

covered). The acquired parameters of interest for each studied sample are presented in Table 1 (modern fibres), Table 2 (ethnographic fibres) and Table 4 (archaeological fibres).

### The modern (reference) fibres

Table 1. The obtained average crystallite widths, relative crystallinities and mean microfibril angles (MFA) obtained for the studied modern fibres.

Sample	Fibre type	Crystal width[nm] ± 0.2 nm	Relative crystallinity (%) ± 5%-unit	MFA (°) ± 1 °
Root A	Flax	4.6	37	12
Crown A	Flax	4.5	34	8
Stem B	Flax	4.1	36	11
Root C	Nettle	3.7	34	19
Stem C	Nettle	4	33	12
Crown C	Nettle	3.4	39	8
Stem D	Nettle	3.9	33	11
Root E	Nettle hyb.	3.7	32	12
Stem E	Nettle hyb.	3.6	32	12
Crown E	Nettle hyb.	3.6	31	12
Stem F	Nettle hyb.	3.6	28	15
Root G	Hemp	4.4	24	13
Root H	Hemp	3.9	29	14
Root I	Hemp	3.7	33	14
Stem J	Hemp	4.8	29	14

For the modern fibres, the obtained average crystallite widths ranged from 3.4 nm to 4.8 nm, the accuracy of results being 0.2 nm. On the average, the obtained crystallite width was smallest in the nettle samples (range 3.4 nm - 4.0 nm) compared to values obtained for flax and hemp (range 4.1-4.6 and 3.7 -4.8 nm, respectively).

The relative crystallinity values obtained for modern fibres were all between 24 - 34% (± 5%-units), showing an ascending order from hemp (24 - 33%) to nettle (28 – 34%), finally to flax with the highest acquired crystallinity values (34 - 37%). Examples of the WAXS patterns and crystallinity fits of the samples are presented in figures 4 (Nettle), 5 (Hemp) and 6 (Flax).

In the case of the microfibril angles, small mean MFA values for all species and samples were detected. The acquired mean MFA values for nettle samples ranged from 8° to 19° and for flax samples from 8° to

12°. In the case of hemp, the obtained MFA values were similar and around 14°.

In addition to the WAXS pattern of cellulose, in the 2D scattering images of modern nettle and hemp fibres, bright diffraction spots with high relative intensities were detected. The possible origin and significance of these observations is covered in the Discussion section.

### The ethnographic (White Karelian textile) fibres

Table 2. The average crystallite widths and relative crystallinities obtained for ethnographic fibres, extracted from the White Karelian textiles. \*(Suomela et al. 2020)

Sample	Fibre type*	Crystal width[nm] ± 0.2 nm	Relative crystallinity (%) ± 5 %-unit
Sample 2a	Nettle	5.3	68
Sample 5a	Flax	7	62
Sample 9b	Nettle	6.9	68
Sample 48b	Flax	6.3	53
Sample 49a	Flax	6	50
Sample 73ba	Hemp	6.5	51
Sample 85d	Nettle	6	48

Table 3. The average crystallite widths obtained for ethnographic cotton fibres, extracted from the White Karelian textiles.

Sample	Crystal width[nm] ± 0.2 nm
Sample 1a	7.5
Sample 1d	7.8
Sample 82c (blue)	7.5
Sample 82c (orange)	6.8
Sample 85a	6.6
Sample 95b (red)	6.4
Sample 99c (blue)	6.9

For the White Karelian fibres of flax, nettle and hemp, the average crystallite widths ranged from 5.3 nm to 7 nm (Table 2). For the cotton fibre samples from the same collection, the average crystallite width ranged from 6.4 nm to 7.8 nm (Table 3).

The relative crystallinity values of the cellulose in the ethnographic fibres of flax, nettle and hemp were determined to be between 48% and 68%. Example of the crystallinity fit along with the 2D scattering image for a garment nettle fibre is presented in figure 7.

### The archaeological (Ravattula Ristimäki) fibres

Table 4. The obtained average crystallite widths obtained for the archaeological fibre samples from Ristimäki in Ravattula. For clarification reasons, the samples are referred in descending order as Ravattula TYA 912, Ravattula TYA 933 and Ravattula TYA 914 within the text.

Sample	Crystal width[nm]
TYA 912:523D	6.1± 0.5 nm
TYA 933:214:9:50	7± 0.2 nm
TYA 914:1607:8A	5.6± 0.2 nm

For all the Ravattula archaeological samples, the main reflections of cellulose I $\beta$  (*110*, *1-10*, *200*, *004*) were observed in the WAXS patterns (Nishiyama et. al., 2002), thus verifying the preservation of cellulose crystals. Using the scattering patterns, it was possible to obtain the average crystallite widths as the cellulose *200* reflection was strongly observable in all three measured samples, which are all presented in figure 8.

For samples TYA 914 and TYA 933, despite the small amount of the sample material, it was possible to generate the average crystallite widths by using the curve fitting method (described in the Methods section). Only for the sample TYA 912, the average crystallite width was manually estimated by using the Scherrer equation, as the fitting of the Gaussian peaks did not produce reliable results due to low scattering intensities observed (see figure 8D). Thus, the error margin for this result is different from the other two.

## Discussion

Samples consisting of modern, ethnographic and archaeological fibres were measured using WAXS to determine the average cellulose crystallite width and relative crystallinity index for the fibre samples. Transmission and polarization light microscopies were also used to reveal the individual and cross-sectional microscale structural features as well as the fibrillar orientation (S/Z-twist) of the chosen ethnographical fibre samples representing each bast fibre type of this study.

### *Microscope studies*

Problems of microscopy method-based identification of bast fibres are discussed widely, see Suomela et al. 2018, 2020; Haugan and Holst, 2014; Lukesova and Holst 2020. There are subjectivity issues in interpretation of longitudinal, cross-sectional as well as the modified Herzog test images.

Also, the absence or presence of calcium oxalate crystals in the fibre surrounding tissues as a conforming identification feature is challenging as if the studied fibres are old or thoroughly processed, it is highly possible that the crystal containing tissues are no longer present. As mentioned by Bergfjord and Holst (2010), in case of archaeological samples, the crystals may be in such fragmented state that they are no longer visible or identifiable. Thus plasma-ashing and further analysing with SEM are suggested (Jakes and Mitchell 1996). However, SEM and plasma-ashing are destructive methods which in general make them less desirable to be used for valuable archaeological samples. As a non-destructive method, XRD offers a way to study nanosized mineral crystallites; especially if the weight fraction of the mineral among the sample is high enough.

Based on the literature, it can also be hypothesized that the cellulose formed crystalline structures are the most intact parts of the archaeological plant samples (Atalla and VanderHart 1984; Hearle et al. 1998; Han et al. 2020). Thus, XRD offers an important additional characterization tool besides light microscopy methods.

### ***WAXS results on modern fibres***

Based on the WAXS results, the average crystallite widths among the modern fibres varied from 3.4 nm to 4.8 nm. It should be noted that the values of the crystallite widths varied significantly within the same plant species. This variation is most likely explained by the natural variation of the growth within biological systems.

For flax and hemp, the obtained average crystallite widths are very similar compared to values acquired in the earlier XRD studies: around 4.5 nm by (Duchemin et al. 2012), and 3.9 nm by (Leppänen et al. 2009) were obtained for flax fibres, and 4.8 nm by (Virtanen et al. 2012) for hemp, (all the values analyzed from the cellulose *200* reflection).

In the case of mean MFA, the obtained values ranged from 8 ° to 19 ° within all the studied modern fibres. For flax and hemp, the obtained MFA values, 8-12 ° and 13 to 14 ° respectively, are similar than the reported values of 8-11 ° in (Bourmaud et al. 2013, Astley & Donald 2001, Placet et al. 2011). No earlier data of the average crystallite widths or MFAs in the case of stinging nettle can be found from the literature. Based on the good agreement between our data and earlier results on the average crystallite widths and MFA of flax and hemp, the obtained values for stinging nettle are reliable and convincing.

In the case of relative crystallinity in flax and hemp fibres, higher values have been obtained in earlier studies (Duchemin et al. 2012; Thygesen et al. 2005). Higher crystallinity index is also obtained for stinging nettle fibres in earlier studies of (Kumar and Das 2017a), in which the relative crystallinity value was determined to be approximately 66 %.

The chosen analysis method for obtaining the (relative) crystallinity affects to the crystallinity value. In all the above-mentioned papers, the authors have used *Segal peak height*-method (Segal et al. 1959) to obtain the crystallinity values for their fibre samples, and it is shown to produce too high crystallinity values compared to other analysis methods (Park et al. 2010; Ahvenainen et al. 2016). In our study, the

relative crystallinities were calculated using *amorphous fitting*-method, which is found to produce more reliable crystallinity values (Ahvenainen et al. 2016).

As mentioned in the results section, another interesting feature in all the measured modern samples of nettle and hemp, are the crystallite deposits (other than cellulose) present based by the 2D scattering patterns. These deposits are revealed by the bright diffraction spots and Debye rings, and are noted also in the integrated scattering intensity curves as sharp peaks (spotted by arrows, Figures 4 and 5). The single bright spots are caused by individual single crystals. Debye rings are detected when the studied material contains these types of crystals in large quantities, isotopically distributed in all possible orientations (i.e., powder-like) throughout the sample.

Most notably, for all the measured modern nettle samples, both bright spots and Debye rings were present in all the scattering patterns. The Debye rings are especially of interest in this case as they suggest that the density and distribution of the crystals responsible for the rings are somewhat constant (with powder like distribution) throughout the measured sample. For the hemp samples, only bright spots (arising from single crystals) were observed as shown in Figure 5. The compounds could potentially be Ca and Si-based due to their great abundance in plant material overall (Burchi et al. 2014) (see Figure S1, supplementary).

The properties of these crystal deposits, e.g., the relative intensity, amount and number density of the diffraction peaks, are higher in all the scattering patterns obtained for the nettle samples compared to hemp samples. The crystallite deposits are assumed to be the single crystals or clusters formed of different compounds of calcium carbonates and oxalates (Fengel and Wegener 1983; Webb 1999).

For all the flax samples, similar clear intensity maxima due to the crystal deposits (excluding crystalline cellulose spectra) were not detected in the scattering patterns. This corresponds to the hypothesis based on earlier PLM results in the literature that the cellular tissue of flax does not contain observable crystal deposits (Catling and Grayson 1982). However, it must be noted, that the absence of these crystals in the case of XRD might be caused by the fact that the relative amount of the crystal compounds is too low to be detected.

### ***WAXS results on White Karelian ethnographic fibres***

The White Karelian fibres of flax, nettle and hemp show significantly higher crystallite widths (5.3 – 7 nm) and crystallinity values (48 – 68 %) compared to the modern fibres extracted from the same species.

One possible explanation to the larger crystallite size and crystallinity compared to those of the modern fibres is the mechanical and/or chemical treatments of the fibres connected to the textile making process, wear and care. Certain chemical compounds, e.g., strong bases or acids, and mechanical processes, i.e., milling, and sun light are known to break the amorphous compounds within the plant material (Hearle et al. 1998, Dadashian et al. 2001; Lionetto et al. 2012; Castro et al. 2011). This can cause the remaining cellulose chains to aggregate as has been observed previously in the case of much stronger chemical treatments as kraft and sulphite pulping and acid hydrolysis (Leppänen et al. 2009; Virtanen et al. 2011).

The increase in the relative crystallinity of cellulose in fibres due to alkali treatment has been observed earlier also in nettle (Kumar and Das 2017a) and hemp (Sawpan et al. 2011). In the case of flax, only a slight increase in the crystallinity index and the average crystallite widths due to alkali treatment has been observed (Cao et al. 2012).

However, it should be noted that the culturohistorical materials in this study are from the time periods when textiles were produced with craft methods. The fibres were most likely first retted and dried, and afterwards commonly braked and stripped to remove the woody xylem of the plant. In the case of nettle, it is also possible that the xylem was removed already from the fresh plants. In the retting process the fibres are separated from other plant tissues with the aid of moisture and micro-organisms. Properly done, it does not affect the highly crystalline bast fibres, but dissolves lignin (Hearle et al. 1998).

Regardless of the used techniques, the fibres have gone through vigorous mechanical processes, both in textile manufacturing and care. We cannot say much about the laundry methods in the Late Bronze Age, but in 19<sup>th</sup> century it was common to use some alkali strong base compounds, e.g., potassium carbonate and sodium hydroxide for washing purposes. Lye was traditionally produced from birch ashes and laundries were boiled and pound in it before twisting in running water (Vilkuna 1943).

Additionally, the studied fibres were most likely exposed to direct sunlight for bleaching purposes. Bast fibres obtain their brownish colour from lignin and traditional practices, ready textiles or cloths were bleach in sunlight with intention to break the lignin structures. In photo-oxidation (Tímar-Balázsy and Eastop 1998), in addition to lignin dissolution, certain wavelengths of ultraviolet radiation are known to break the amorphous cellulosic compounds in different plant materials, leading to higher relative crystallinity of the remaining cellulose (Hearle et al. 1998, Dadashian et al. 2001; Lionetto et al. 2012).

### ***WAXS results on Ravattula archaeological fibres***

The obtained crystallite widths for Ravattula samples are similar within the error limits (5.6 – 6.1 nm) compared to the values obtained for the ethnographic samples 2a, 85d, 48b and 49a, which might be explained by the fact that the Ravattula fibres are probably extracted from the same species of plants (nettle, hemp or flax), and treated with roughly similar kinds of treatments.

Apart from the results on crystallite width and relative crystallinity, the 2D scattering images can provide information about the possible degradation of the cellulose and the mechanical treatments conducted on the fibre, e.g., the textile fibre twisting. The azimuthal integral was used to determine the cellulose microfibrillar orientation in the form of the microfibril angle in the case of native fibres. However, for the Karelian and Ravattula fibres this kind of fibrillar orientation could not be determined similarly, because depending on the bundle sizes of the fibre samples, the cellulose 200 reflection can be broadened in the azimuthal direction due to various factors. One possible explanation for the azimuthal broadening is that the studied fibre material has gone through some sort of fibre twisting-procedure. For the archaeological samples TYA912 and TYA914, the observed reflections in the 90-degree azimuthal periods are connected to the fabrics structure.

Overall, the ability to observe the cellulose reflections, especially in the samples TYA 912 and TYA 914, shows the low degradation rate of the cellulose within the fibres. This is quite surprising because there are not many well-preserved archaeological plant-fibre samples from different textiles from 11<sup>th</sup> century found from Finland due to the acidic soil type (Riikonen 2011).

The archaeological samples were associated with metal containing objects, which has potentially helped the preservation of the fibres. The possible mineralization could be observed from the 2D scattering images as they have many clear Debye rings which might arise from the metallic oxides, reasonably from copper containing compounds (Fig. 8 A, B and C). Some of the common compounds ( $\text{CuCl}$ ,  $\text{CuCl}_2$ ,  $\text{CuO}_2$  and  $\text{Cu}_2\text{CO}_3$ ) identified in earlier studies (Reynaud et al. 2020) were presented with the integrated scattering curves (see Fig. 8D). It has been observed earlier that close contact with metal items promotes the conservation of textile fibres by preventing microbial activity (Janaway 1987). The corrosion process releases metal ions which impregnate the fibre partially or fully, creating a pseudomorph. In addition to microbial activity, acidic soil, which is common in Finland, degrades cellulose based fibres through acid-based hydrolysis (Hearle et al. 1998). Therefore, the textile finds from Finland are often linked to metal artefacts.

Moreover, the scattering data of this study on the archaeological samples emphasized the fact that a synchrotron facility is not necessarily needed to study archaeological fibre samples. Crucial information about the ultrastructural properties of these types of fibres can be obtained also by using home laboratory WAXS equipment.

### ***Comparison of the results for all fibres***

Based on the results for the cellulose crystallite widths obtained for all the samples, the different bast fibre types (hemp, flax or nettle) cannot be distinguished from each other. This is in line with the earlier conclusions presented by also Müller et al. regarding archaeological fibres of the same type, hemp/flax/ramie (Müller et al. 2004, 2007). They presented that only cotton fibres can be distinguished indisputably from all the other bast fibres.

In the present study, in the studied historical cotton fibre samples, the average cellulose crystallite widths were similar compared to the other historical fibre types studied. So, it could be noted here, that the cellulose crystallite widths were determined to be significantly larger for all the historical/archaeological fibre samples compared to the crystallite widths of recent fibres. As such this is a highly interesting observation and result.

Even though the cellulose crystallite width does not provide information to be used in the fibre identification, the whole 2D scattering patterns provide potential tool for the identification purposes. The scattering patterns of modern nettle fibres had features which were not present in any other studied modern fibres: the Debye rings arising from the powder like distribution of plant mineral crystals. However, these same features were not present in the ethnographic or archaeological nettle fibres,

suggesting that some of the possible treatments of the textiles have removed these mineral crystal deposits from the fibres.

Based on our observations and the results within the set of studied fibres, the Debye rings could potentially be used as an indication of the fibre type and condition. With the Debye rings present in the 2D WAXS patterns, it is possible to distinguish fibres with the same crystallite width, i.e., nettle fibres from cotton, as the mineral compounds (possible Si or Ca compounds) responsible of the rings are only present in nettle. Furthermore, this information could potentially be useful for criminal investigation purposes as well as for historical research concerning nettle textiles and fibres.

## Conclusions

In this study, modern, ethnographical and archaeological fibre samples of flax, hemp and nettle were studied using Wide-angle X-ray Scattering and polarization and transmission light microscopies. The scattering patterns of crystalline cellulose were observed in all the archaeological fibre samples, thus revealing the presence of crystalline cellulose in significant amounts in these samples.

By using the WAXS data, the ultrastructural features of modern nettle fibres were determined and compared to the corresponding values of flax and hemp, which has not been done previously. The average cellulose crystallite width in the modern nettle fibres was 3.7 nm, which was slightly smaller than the average crystallite widths of flax (4.4 nm) and hemp (4.2 nm). However, the variability between the individual fibre samples was of the same scale than the differences between these species. The cellulose crystallite widths and relative crystallinities were significantly larger in all the historical and archaeological fibre samples studied. The scattering patterns of modern nettle fibres also revealed the presence of other crystalline compounds, presumably different compounds of Ca and Si, which were seemingly abundant throughout the measured nettle fibre samples. These features were not observed in any other fibre type of this study. This observation could potentially be further utilized to identify modern nettle fibres from flax, hemp and cotton.

## Declarations

### Acknowledgements

*K.S. and M.V. acknowledge the University of Helsinki (3-year research grant).*

J.S. acknowledge the grant from Karjalaisen Kulttuurin Edistämissäätiö.

We acknowledge the provision of facilities and technical support by Aalto University at OtaNano - Nanomicroscopy Center (Aalto-NMC)

We would like to thank Ville Heiskanen from the Botanical Gardens of University of Helsinki, in Kumpula; Jaana Riikonen and Juha Ruohonen from the University of Turku; and Ildikó Lehtinen and Anna-Mari Immonen from the National Museum of Finland.

## Declarations

## Funding

This study was funded by the *University of Helsinki 3-year research grant*.

## Conflicts of Interest

The authors declare that they have no competing interests.

## Availability of data and material

Data is available upon request.

## Code availability

All the custom scripts used in data-analysis are available upon request.

## Authors' contributions

M.V. and K.S. carried out the scattering experiments. J.S. carried out the optical microscopy measurements. M.V. wrote the manuscript with support from J.S. and K.S. All the authors conceived the original idea.

## Ethics approval

Not applicable

## Consent to participate

Not applicable

## Consent for publication

Not applicable

## References

- Ahvenainen, P., Kontro, I., & Svedström, K. (2016). Comparison of sample crystallinity determination methods by X-ray diffraction for challenging cellulose I materials. *Cellulose*, *23*(2), 1073–1086. <http://dx.doi.org/10.1007/s10570-016-0881-6>
- Andersson, S., Serimaa, R., Paakkari, T., Saranpää, P., & Pesonen, E. (2003). Crystallinity of wood and the size of cellulose crystallites in Norway spruce (*Picea abies*). *Journal of Wood Science*, *49*(6), 531-537. <http://dx.doi.org/10.1007/s10086-003-0518-x>
- Astley, O.M. & A.M. Donald. (2001). A Small-Angle X-ray Scattering Study of the Effect of Hydration on the Microstructure of Flax Fibers. *Biomacromolecules*, *2*(3), 672-680. <https://doi.org/10.1021/bm005643l>
- Atalla, R. H., & Vanderhart, D. L. (1984). Native cellulose: a composite of two distinct crystalline forms. *Science*, *223*(4633), 283-285. <http://dx.doi.org/10.1126/science.223.4633.283>

- Bergfjord, C., & Holst, B. (2010). A procedure for identifying textile bast fibres using microscopy: flax, nettle/ramie, hemp and jute. *Ultramicroscopy*, *110*(9), 1192–1197.  
<http://dx.doi.org/10.1016/j.ultramic.2010.04.014>
- Bergfjord, C., Mannering, U., Frei, K. M., Gleba, M., Scharff, A. B., Skals, I., ... & Holst, B. (2012). Nettle as a distinct Bronze Age textile plant. *Scientific Reports*, *2*, 664. <http://dx.doi.org/10.1038/srep00664>
- Bourmaud, A., Morvan, C., Bouali, A., Placet, V., Perre, P., & Baley, C. (2013). Relationships between microfibrillar angle, mechanical properties and biochemical composition of flax fibers. *Industrial Crops and Products*, *44*, 343-351. <https://doi.org/10.1016/j.indcrop.2012.11.031>
- Burchi, G., Bauchan, G. R., Murphy, C., & Roh, M. S. (2014). Characterisation of calcium crystals in *Abelia* spp. using X-ray diffraction and electron microscopy. *The Journal of Horticultural Science and Biotechnology*, *89*(1), 61–68. <https://doi.org/10.1080/14620316.2014.11513049>
- Cao, Y., Chan, F., Chui, Y. H., & Xiao, H. (2012). Characterization of flax fibres modified by alkaline, enzyme, and steam-heat treatments. *BioResources*, *7*(3), 4109–4121.
- Catling D. & Grayson J. (1982) Introduction. In: Identification of Vegetable Fibres. Springer, Dordrecht. [https://doi.org/10.1007/978-94-011-8070-2\\_1](https://doi.org/10.1007/978-94-011-8070-2_1)
- Chen, H. L., Jakes, K. A., & Foreman, D. W. (1998). Preservation of archaeological textiles through fibre mineralization. *Journal of Archaeological Science*, *25*(10), 1015–1021.  
<https://doi.org/10.1006/jasc.1997.0286>
- Dadashian, F., & Wilding, M. A. (2001). Photodegradation of lyocell fibers through exposure to simulated sunlight. *Textile Research Journal*, *71*(1), 7–14. <https://doi.org/10.1177/004051750107100102>
- Debnath, S. (2015). Great potential of stinging nettle for sustainable textile and fashion. In *Handbook of sustainable luxury textiles and fashion* (pp. 43-57). Springer, Singapore. [https://doi.org/10.1007/978-981-287-633-1\\_3](https://doi.org/10.1007/978-981-287-633-1_3)
- Deedrick, D. W. (2000). *Hairs, fibres, crime, and evidence: Part 2, fibre evidence*. US Department of Justice, Federal Bureau of Investigation.
- Duchemin, B., Thuault, A., Vicente, A., Rigaud, B., Fernandez, C., & Eve, S. (2012). Ultrastructure of cellulose crystallites in flax textile fibres. *Cellulose*, *19*(6), 1837-1854.  
<http://dx.doi.org/10.1007/s10570-012-9786-1>
- Fengel, D., & Wegener, G. (Eds.). (1983). *Wood: chemistry, ultrastructure, reactions*. Walter de Gruyter. <https://doi.org/10.1515/9783110839654>
- Geijer, A. (1979) *A history of textile art: a selective account*. London: Sotheby Parke Bernet.

- Good, I. (2001). Archaeological textiles: a review of current research. *Annual Review of Anthropology*, 30(1), 209-226. <https://doi.org/10.1146/annurev.anthro.30.1.209>
- Han, L., Tian, X., Keplinger, T., Zhou, H., Li, R., Svedström, K., Burgert, I., Yin, Y., & Guo, J. (2020). Even Visually Intact Cell Walls in Waterlogged Archaeological Wood Are Chemically Deteriorated and Mechanically Fragile: A Case of a 170-Year-Old Shipwreck. *Molecules*, 25(5). <https://doi.org/10.3390/molecules25051113>
- Haugan, E., & Holst, B. (2013). Determining the fibrillar orientation of bast fibres with polarized light microscopy: the modified Herzog test (red plate test) explained. *Journal of microscopy*, 252(2), 159–168. <https://doi.org/10.1111/jmi.12079>
- Haugan, E., & Holst, B. (2014). Flax look-alikes: Pitfalls of ancient plant fibre identification. *Archaeometry*, 56(6), 951–960. <https://doi.org/10.1111/arcm.12054>
- Hearle, J. W., Lomas, B., & Cooke, W. D. (1998). *Atlas of fibre fracture and damage to textiles, Part VIII – Fibre Archaeology and Textile Conservation*. Elsevier.
- Jakes, K., & Mitchell, J. (1996). Cold plasma ashing preparation of plant phytoliths and their examination with scanning electron microscopy and energy dispersive analysis of X-rays. *Journal of archaeological science*, 23(1), 149-156. <https://doi.org/10.1006/jasc.1996.0012>
- Janaway, R. C. (1987). The preservation of organic materials in association with metal artefacts deposited in inhumation graves. In *Death, decay and reconstruction: approaches to archaeology and forensic science* (pp. 127–148). Manchester: Manchester University Press.
- Kumar, N., & Das, D. (2017a). Alkali treatment on nettle fibres: Part I: investigation of chemical, structural, physical, and mechanical characteristics of alkali-treated nettle fibres. *The Journal of The Textile Institute*, 108(8), 1461-1467. <https://doi.org/10.1080/00405000.2016.1257346>
- Kumar, N., & Das, D. (2017b). Fibrous biocomposites from nettle (*Girardinia diversifolia*) and poly (lactic acid) fibers for automotive dashboard panel application. *Composites Part B: Engineering*, 130, 54-63. <https://doi.org/10.1016/j.compositesb.2017.07.059>
- Lanzilao, G., Goswami, P., & Blackburn, R. S. (2016). Study of the morphological characteristics and physical properties of Himalayan giant nettle (*Girardinia diversifolia* L.) fibre in comparison with European nettle (*Urtica dioica* L.) fibre. *Materials Letters*, 181, 200–203. <https://doi.org/10.1016/j.matlet.2016.06.044>
- Leppänen, K., Andersson, S., Torkkeli, M., Knaapila, M., Kotelnikova, N., & Serimaa, R. (2009). Structure of cellulose and microcrystalline cellulose from various wood species, cotton and flax studied by X-ray scattering. *Cellulose*, 16(6), 999-1015. <https://doi.org/10.1007/s10570-009-9298-9>

Lionetto, F., Del Sole, R., Cannoletta, D., Vasapollo, G., & Maffezzoli, A. (2012). Monitoring wood degradation during weathering by cellulose crystallinity. *Materials*, 5(10), 1910–1922. <https://doi.org/10.3390/ma5101910>

Lukesova, H., & Holst, B. (2020). Is cross-section shape a distinct feature in plant fibre identification?. *Archaeometry*. <https://doi.org/10.1111/arcm.12604>

Markova, I. (2019). *Textile fibre microscopy: A practical approach*. John Wiley & Sons. <https://doi.org/10.1002/9781119320029>.

Müller, M., Murphy, B., Burghammer, M., Riekkel, C., Roberts, M., Papiz, M., ... & Pantos, E. (2004). Identification of ancient textile fibres from Khirbet Qumran caves using synchrotron radiation microbeam diffraction. *Spectrochimica Acta Part B: Atomic Spectroscopy*, 59(10-11), 1669-1674. <https://doi.org/10.1016/j.sab.2004.07.018>

Müller, M., Murphy, B., Burghammer, M., Snigireva, I., Riekkel, C., Gunneweg, J., & Pantos, E. (2006). Identification of single archaeological textile fibres from the cave of letters using synchrotron radiation microbeam diffraction and microfluorescence. *Applied Physics A*, 83(2), 183-188. <https://doi.org/10.1007/s00339-006-3516-1>

Müller, M., Murphy, B., Burghammer, M., Riekkel, C., Pantos, E., & Gunneweg, J. (2007). Ageing of native cellulose fibres under archaeological conditions: textiles from the Dead Sea region studied using synchrotron X-ray microdiffraction. *Applied Physics A*, 89(4), 877-881. <https://doi.org/10.1007/s00339-007-4219-y>

Nayak, R. K., R. Padhye, and S. Fergusson. 2012. "Identification of Natural Textile Fibres." In *Handbook of Natural Fibres*. Vol. 1, edited by R. M. Kozlowski, 314–344. Woodhead Publishing Series in Textiles: Number 118. Oxford: Woodhead. <https://doi.org/10.1016/c2013-0-17333-3>

Nishiyama, Y., Langan, P., & Chanzy, H. (2002). Crystal structure and hydrogen-bonding system in cellulose I $\beta$  from synchrotron X-ray and neutron fiber diffraction. *Journal of the American Chemical Society*, 124(31), 9074-9082. <https://doi.org/10.1021/ja0257319>

Park, S., Baker, J. O., Himmel, M. E., Parilla, P. A., & Johnson, D. K. (2010). Cellulose crystallinity index: measurement techniques and their impact on interpreting cellulase performance. *Biotechnology for biofuels*, 3(1), 10. <https://doi.org/10.1186/1754-6834-3-10>

Placet, V., Bouali, A., Perré, P. (2011). The possible role of microfibril angle of Hemp fibre during fatigue tests and its determination using Wide-Angle X-ray diffraction. *Matériaux & Techniques*, 99(6),683-689. <https://doi.org/10.1051/mattech/2011120>

Ramamoorthy, S. K., Skrifvars, M., & Persson, A. (2015). A review of natural fibres used in biocomposites: plant, animal and regenerated cellulose fibres. *Polymer Reviews*, 55(1), 107–162.

<https://doi.org/10.1080/15583724.2014.971124>

Reiterer, A., Lichtenegger, H., Tschegg, S., & Fratzl, P. (1999). Experimental evidence for a mechanical function of the cellulose microfibril angle in wood cell walls. *Philosophical Magazine A*, 79(9), 2173–2184. <https://doi.org/10.1080/01418619908210415>

Reynaud, C., Thoury, M., Dazzi, A., Latour, G., Scheel, M., Li, J., ... & Bertrand, L. (2020). In-place molecular preservation of cellulose in 5,000-year-old archaeological textiles. *Proceedings of the National Academy of Sciences*, 117(33), 19670-19676. <https://doi.org/10.1073/pnas.2004139117>

Riikonen, J. (2011). "White Linen: Cloth of Luxury." In *Times, Things & Places: 36 Essays for Jussi-Pekka Taavitsainen*, edited by J. Harjula, M. Helamaa, and J. Haarala, 198–221. Masku: J.-P. Taavitsainen Festschrift Committee.

Ruohonen, J. (2017). Ristimäki in Ravattula: On the remains of the oldest known church in Finland. In Harjula & Hukantaival (eds.) *New Visits to Old Churches: Sacred Monuments and Practices in the Baltic Sea Region*, Cambridge Scholars Publishing, 46-60.

Sanjay, M. R., Siengchin, S., Parameswaranpillai, J., Jawaid, M., Pruncu, C. I., & Khan, A. (2019). A comprehensive review of techniques for natural fibers as reinforcement in composites: Preparation, processing and characterization. *Carbohydrate polymers*, 207, 108-121. <https://doi.org/10.1016/j.carbpol.2018.11.083>

Sarén, M-P., Serimaa, R., Andersson, S., Saranpää, P., Keckes, J., Fratzl, P. (2004). Effect of growth rate on mean microfibril angle and cross-sectional shape of tracheids of Norway spruce. *Trees*, 18(3), 354-362. <https://doi.org/10.1007/s00468-003-0313-8>.

Sawpan, M. A., Pickering, K. L., & Fernyhough, A. (2011). Effect of various chemical treatments on the fibre structure and tensile properties of industrial hemp fibres. *Composites Part A: Applied Science and Manufacturing*, 42(8), 888–895. <https://doi.org/10.1016/j.compositesa.2011.03.008>

Segal, L. G. J. M. A., Creely, J. J., Martin Jr, A. E., & Conrad, C. M. (1959). An empirical method for estimating the degree of crystallinity of native cellulose using the X-ray diffractometer. *Textile research journal*, 29(10), 786–794. <https://doi.org/10.1177/004051755902901003>

Sfiligoj S., M., Hribernik, S., Stana Kleinschek, K., & Kreže, T. (2013). Plant fibres for textile and technical applications. *Advances in agrophysical research*, 369-398. <https://doi.org/10.5772/52372>

Svedström, K., Bjurhager, I., Kallonen, A., Peura, M., & Serimaa, R. (2012). Structure of oak wood from the Swedish warship Vasa revealed by X-ray scattering and microtomography. *Holzforschung*, 66(3), 355–363. <https://doi.org/10.1515/hf.2011.157>

Suomela, J. A., Vajanto, K., & Räisänen, R. (2018). Seeking Nettle Textiles—Utilizing a Combination of Microscopic Methods for Fibre Identification. *Studies in Conservation*, 63(7), 412–422.

<https://doi.org/10.1080/00393630.2017.1410956>

Suomela, J. A., Vajanto, K., & Räisänen, R. (2020). Examining the White Karelian Textile Tradition of the Late Nineteenth Century—Focus on Plant Fibres. *Textile*, TEXTILE, 18:3, 298 -324.

<https://doi.org/10.1080/14759756.2019.1699365>

Tímár-Balázsy, Á., & Eastop, D. (1998). *Chemical principles of textile conservation*. Oxford: Butterworth-Heinemann. <https://doi.org/10.4324/9780080501048-25>

Thygesen, A., Oddershede, J., Lilholt, H., Thomsen, A. B., & Ståhl, K. (2005). On the determination of crystallinity and cellulose content in plant fibres. *Cellulose*, 12(6), 563. <https://doi.org/10.1007/s10570-005-9001-8>

Vajanto, K. (2014). Finnish Shipwreck Textiles from the 13th–18th Centuries AD. *Monographs of the Archaeological Society of Finland 3: Focus on Archaeological Textiles: Multidisclipinary Approaches*, 116-131.

Viju, S., & Thilagavathi, G. (2020). Characterization of surface modified nettle fibers for composite reinforcement. *Journal of Natural Fibers*, 1–9. <https://doi.org/10.1080/15440478.2020.1788491>

Vilkuna, K. (1943). *Isien työt 1 – Veden ja maan vilja*. Helsinki: Otava.

Virtanen, T., Svedström, K., Andersson, S., Tervala, L., Torkkeli, M., Knaapila, M., ... & Serimaa, R. (2012). A physico-chemical characterisation of new raw materials for microcrystalline cellulose manufacturing. *Cellulose*, 19(1), 219–235. <https://doi.org/10.1007/s10570-011-9636-6>

Webb, M. A. (1999). Cell-mediated crystallization of calcium oxalate in plants. *The plant cell*, 11(4), 751–761). <https://doi.org/10.1105/tpc.11.4.751>

## Tables

Due to technical limitations, the tables are only available as a download in the supplemental files section.

## Figures

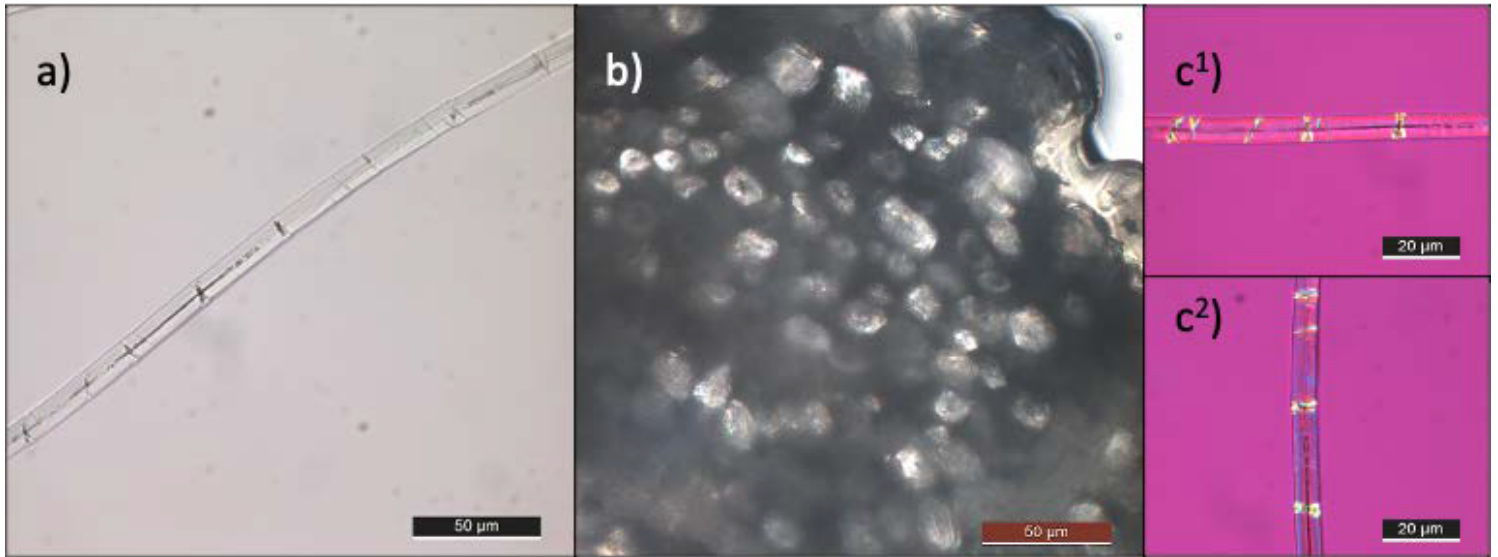


**Figure 1**

TLM and PLM images of the White Karelian flax fibre 5a.

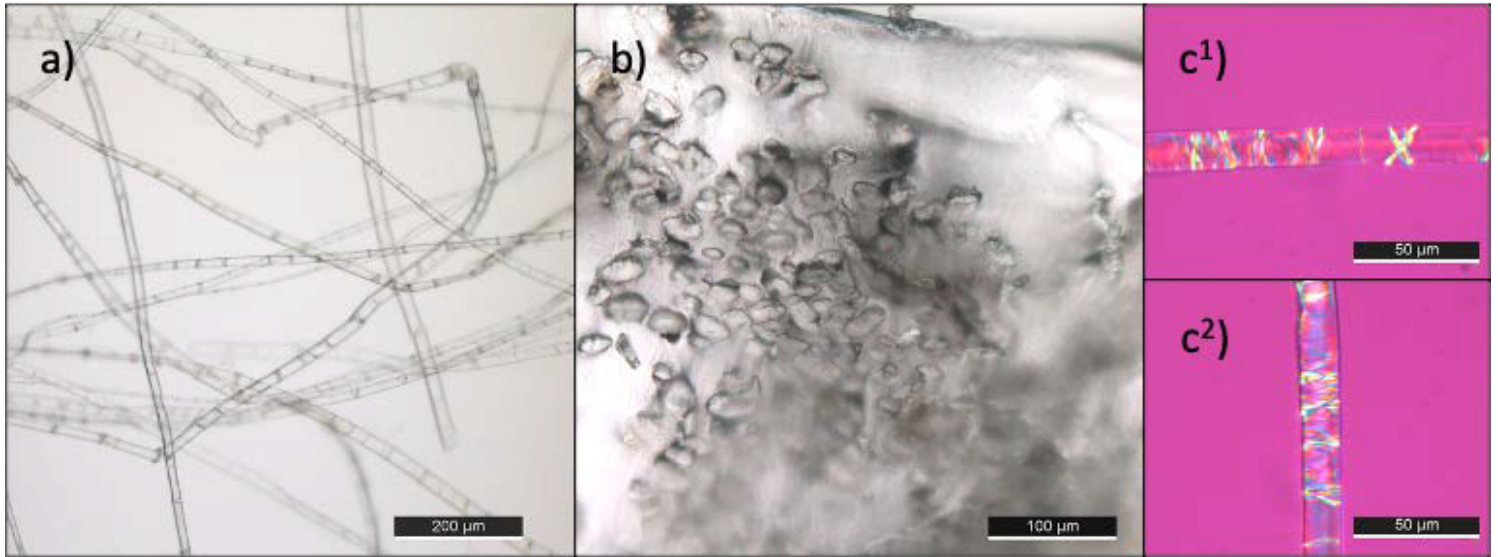


**Figure 2**

TLM and PLM images of the White Karelian nettle fibre 9b.

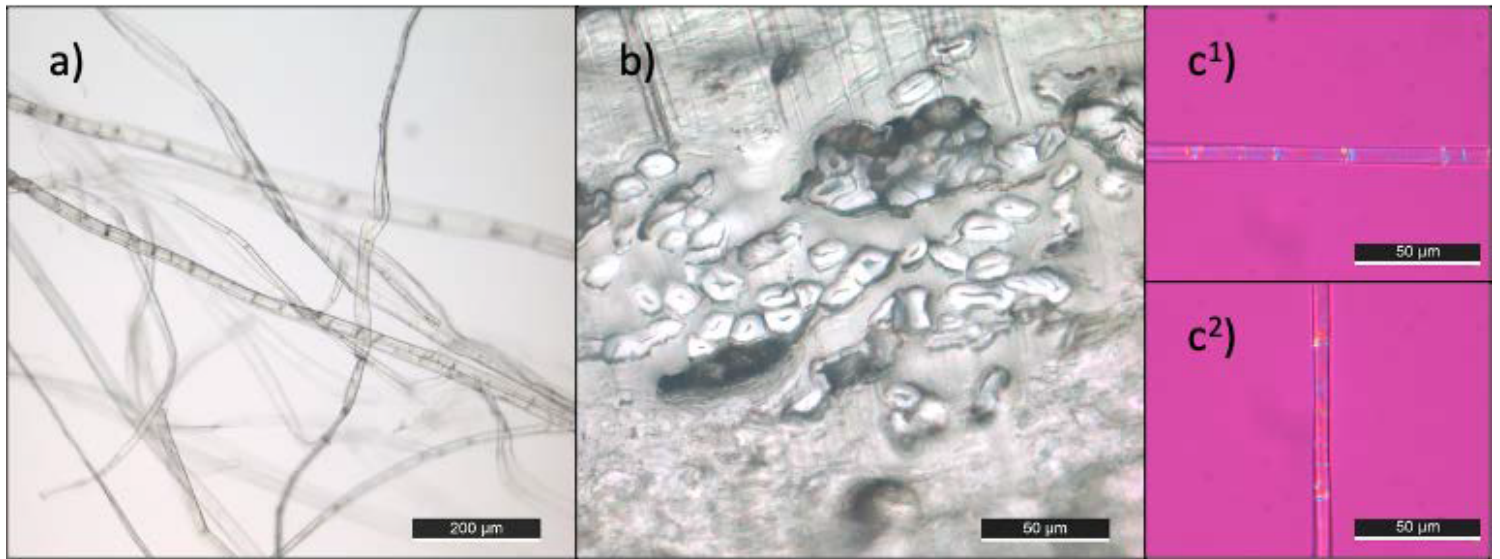


**Figure 3**

TLM and PLM images of the White Karelian hemp fibre 73ba.

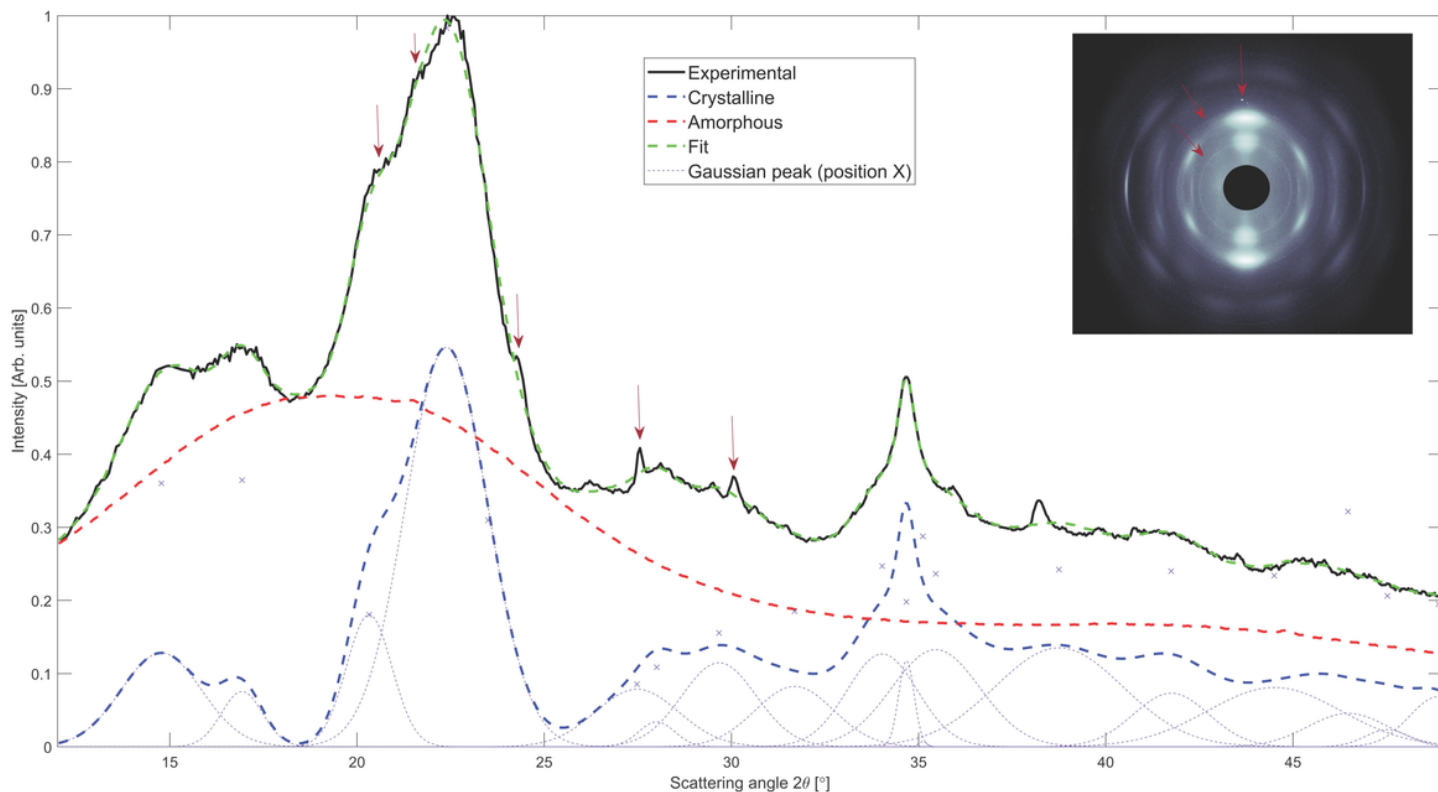


**Figure 4**

The crystallinity fit of the modern reference stinging nettle sample Root C with the 2D scattering image of the same sample. The data used in the crystallinity analysis has been integrated from the 180°-wide sector around the upmost 200 reflection of cellulose. The crystallite deposits are marked with red arrows. As can be detected here, the crystallinity analysis considers only the cellulose reflections indicated with grey dashed line (i.e., the obtained result is the amount of crystalline cellulose among the whole sample).

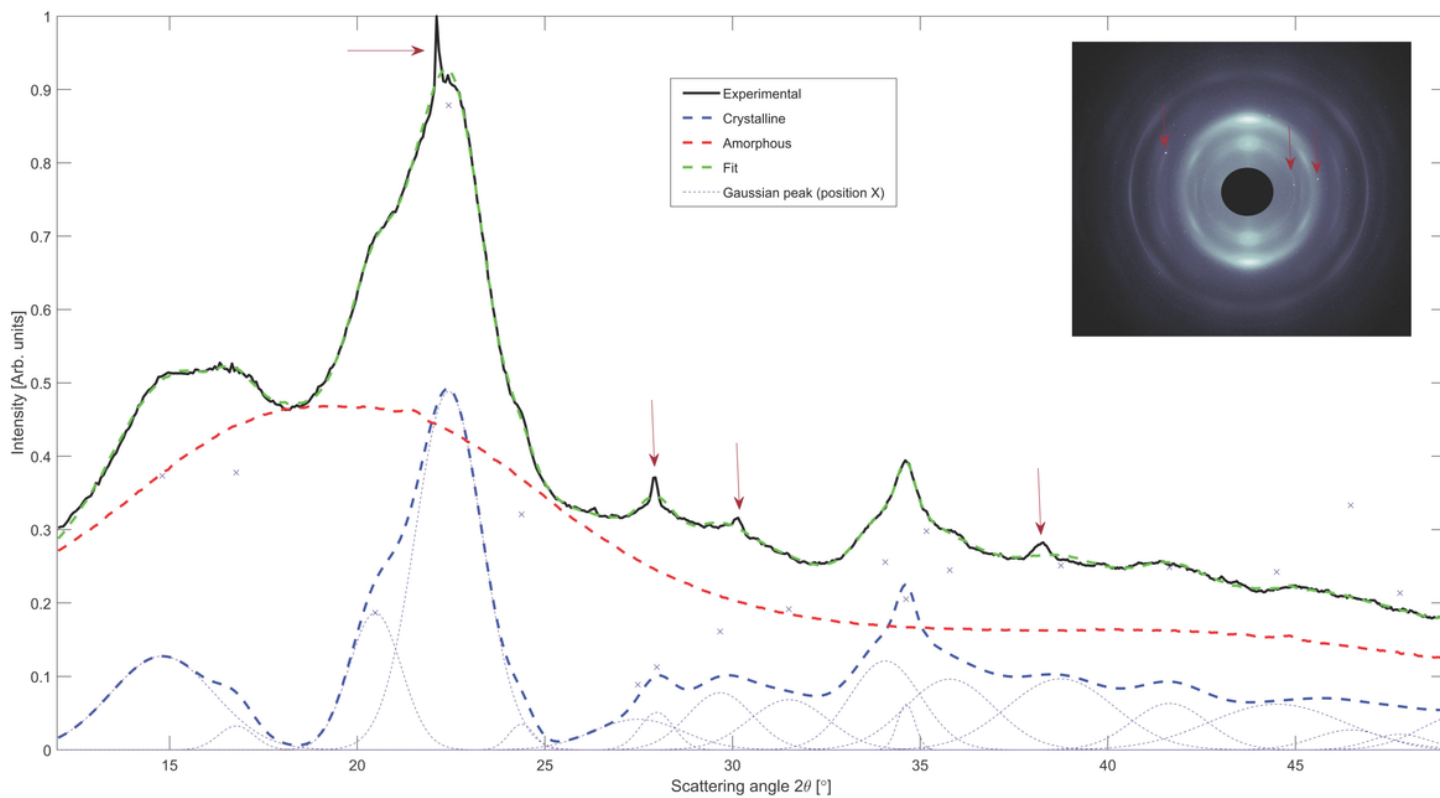


**Figure 5**

The crystallinity fit of the modern reference hemp sample Root H with the 2D scattering image of the same sample. The data for the crystallinity analysis has been integrated from the same sector as for the nettle sample in Fig. 4. The reflections of crystallite non-cellulose deposits are marked with red arrows.

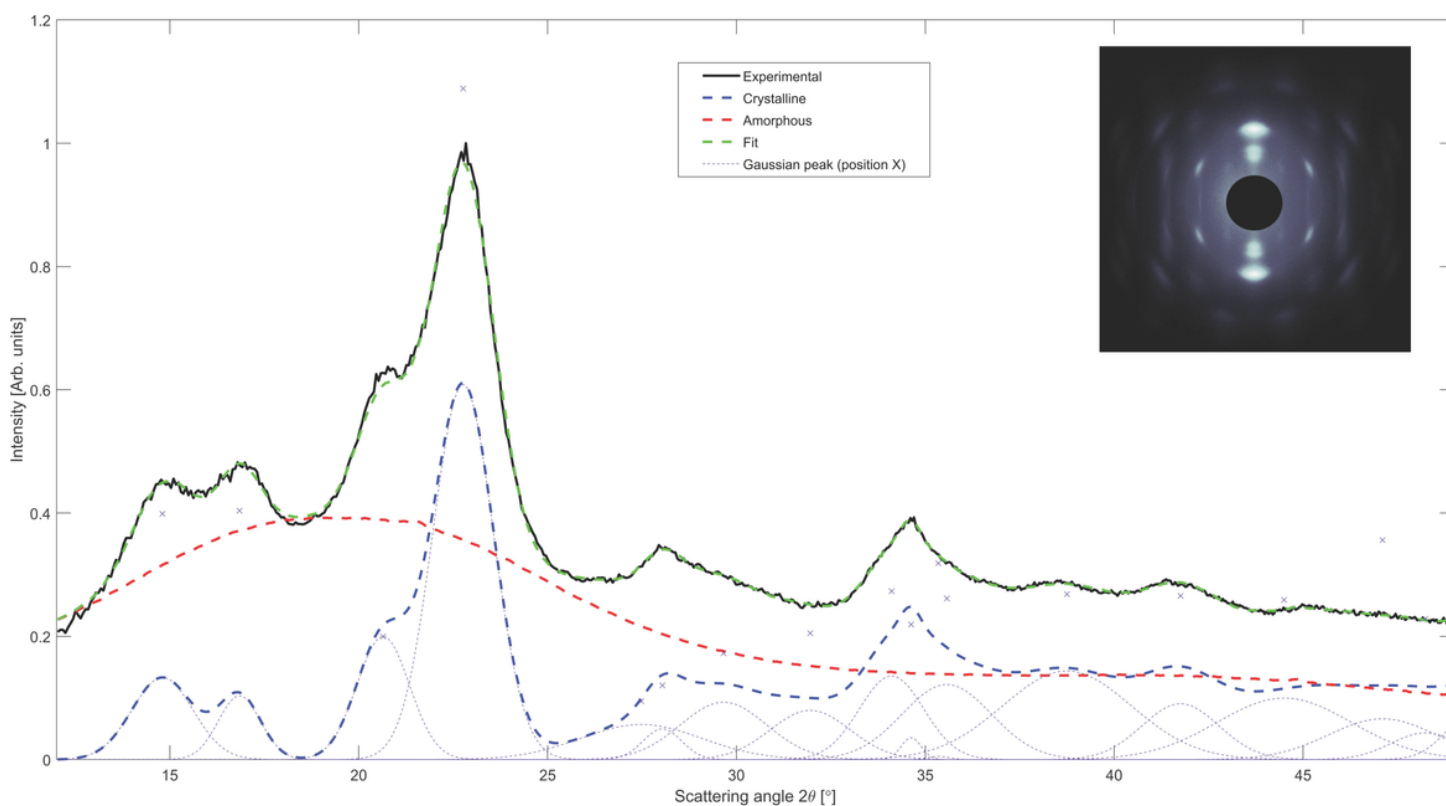


**Figure 6**

The data for the crystallinity analysis has been integrated from the same sector as for the nettle sample in Fig. 4.

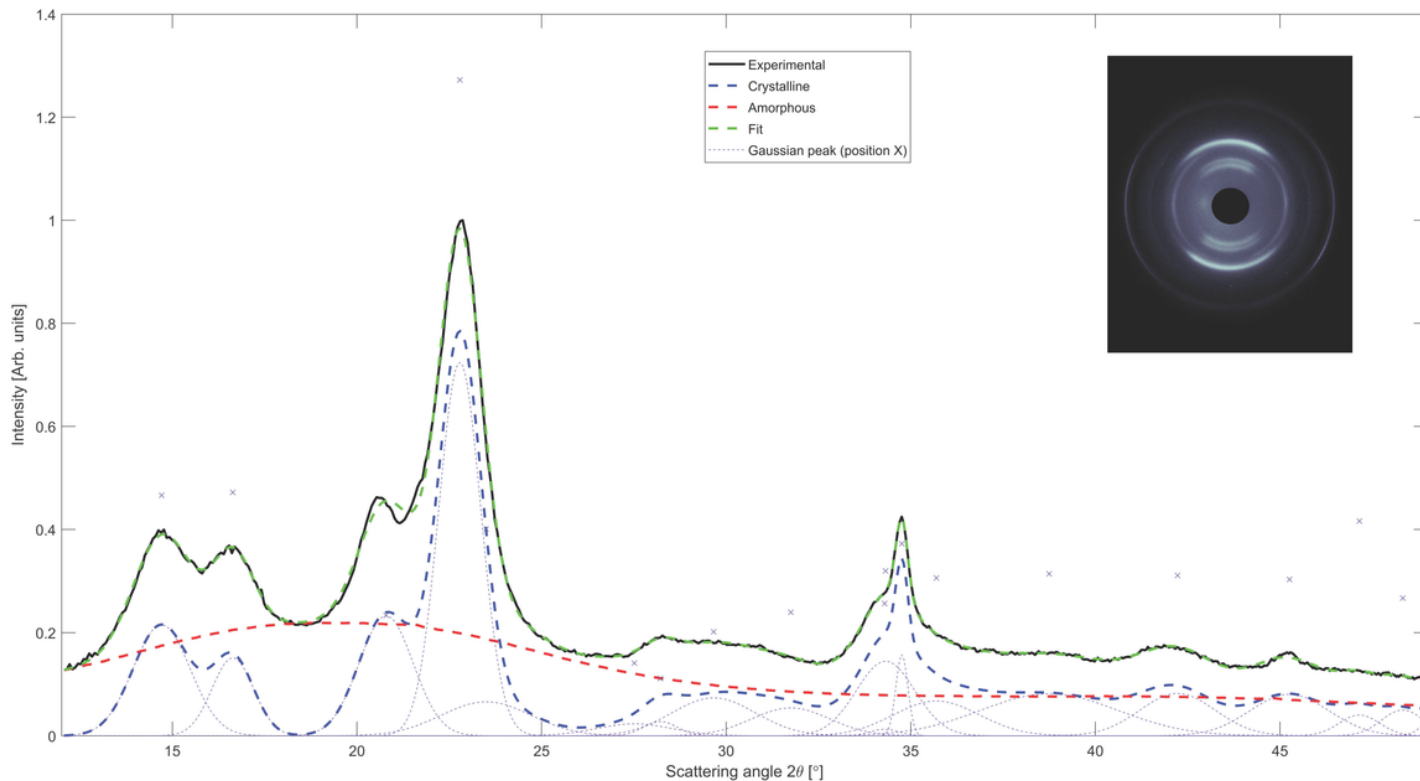


**Figure 7**

The crystallinity fit of the ethnographic nettle sample 85d with the 2D scattering image of the same sample (insert). The data used in the crystallinity analysis has been integrated from the 180°-wide sector around the upmost 200 reflection of cellulose.

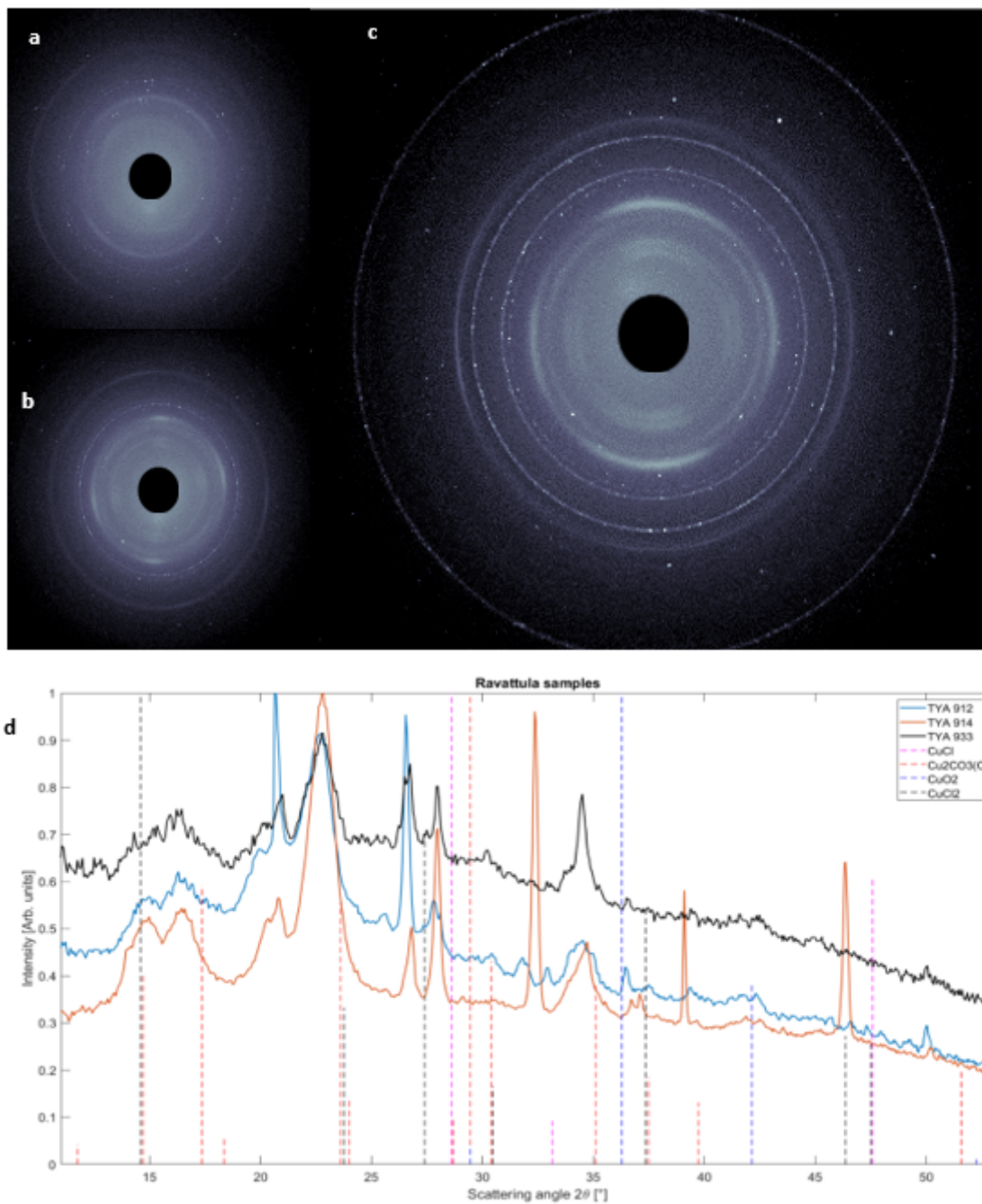


**Figure 8**

The 2D scattering images of Ravattula samples. a) 2D image of sample TYA 912, b) 2D image of sample TYA 914, c) scattering image of the sample TYA 933. This sample was in the best condition as the diffraction maxima's for the cellulose are clearly visible. In d) the most common Cu-compounds responsible for mineralization are mapped with the integrated intensities of each sample.

## Supplementary Files

This is a list of supplementary files associated with this preprint. Click to download.

- [Supplementaryinformation.docx](#)
- [Table1.xlsx](#)
- [Table2.xlsx](#)
- [Table3.xlsx](#)
- [Table4.xlsx](#)